A Comparison of Discrete Models of DC-DC Converters

Milovan Kovačević

***Abstract* — In this paper, a comparison of three discrete models of DC-DC converters is presented. The methods considered are forward Euler, backward Euler, and trapezoidal rule. Results obtained from continuous model, based on averaging and linearization, and from discrete models are compared. It is shown that behavior of Euler-based discrete models may differ significantly from behavior of continuous model based on averaging and linearization. Trapezoidal-based discrete model and continuous model exhibit almost identical behavior at lower frequencies.**

***Keywords* — averaging, converter, discretization, model, linearization, pole position, transfer function.**

I. Introduction

THE TOPIC of this paper is a comparison of discrete models of DC-DC converters. These models are based on forward Euler, backward Euler, and trapezoidal rule. All results are based on analysis of buck converter, presented in Fig. 1, although the results may be generalized to other types of DC-DC converters.

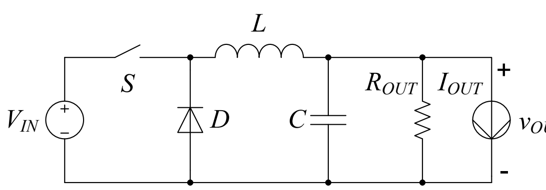

Fig. 1. Electrical circuit of the buck converter.

In this paper, discrete models derived using forward Euler, backward Euler and trapezoidal rules are considered. Their step responses are compared to step response of the continuous model based on averaging and linearization. Also, pole position errors introduced by discretization, as well as basic features of discretization methods, are analyzed and compared for Euler and trapezoidal rules.

II. Averaging and Linearization

Buck converter in Fig. 1 consists of switching network (switch S and diode D) and the output low pass LC filter. Let us assume that DC-DC converter operates in the continuous conduction mode (CCM). Switches considered are ideal and nondisipative. Switch S produces rectangular voltage waveform of duty-ratio D on the input of the low pass filter. The filter removes AC components produces average DC output voltage

$$v_{OUT} \approx \langle v_X \rangle_{T_S} = DV_{IN} \tag{1}$$

where $\langle v_X \rangle_{T_S}$ represents averaged value of v_X within one switching period T_S.

Value of the output DC component is directly proportional to the value of duty ratio D. The switch operation is presented in Fig. 2.

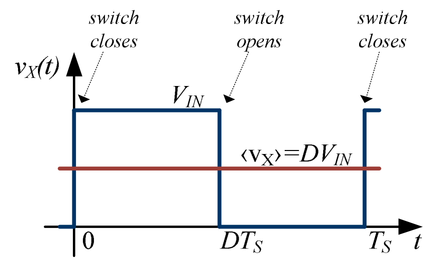

Fig. 2. Switch output voltage $v_X(t)$ (blue) and its average DC value on the output of the low pass filter(red) for D=0.5.

In equilibrium, the capacitor current i_C obeys the ampere-second (As) balance [1] within one switching period

$$\langle i_C \rangle_{T_S} = 0 \,. \tag{2}$$

Similarly, the inductor voltage v_L obeys the voltage-second balance [1] within one switching period

$$\langle v_L \rangle_{T_S} = 0 \,. \tag{3}$$

Otherwise, the converter is not in equilibrium. The average capacitor voltage and the inductor current are obtained as

$$\langle v_C \rangle_{T_S} = \langle v_{OUT} \rangle_{T_S} = DV_{IN} \tag{4}$$

and

$$\langle i_L \rangle_{T_S} = I_{OUT} + \frac{\langle v_{OUT} \rangle_{T_S}}{R} \,. \tag{5}$$

Equations which define the behavior of inductor, capacitor, and resistor remain the same after averaging

$$\langle v_L \rangle_{T_S} = \left\langle L\frac{di_L}{dt} \right\rangle_{T_S} = L\frac{d}{dt}\langle i_L \rangle_{T_S} \,, \tag{6}$$

$$\langle i_C \rangle_{T_S} = C\left\langle \frac{dv_C}{dt} \right\rangle_{T_S} = C\frac{d}{dt}\langle v_C \rangle_{T_S} \,, \tag{7}$$

and

$$\langle v_R \rangle_{T_S} = \langle v_{OUT} \rangle_{T_S} = R\langle i_R \rangle_{T_S} \,. \tag{8}$$

For the switch S and the diode D, however, the equations are simplified by averaging operator

M. Kovačević is graduate student of School of Electrical Engineering, 11120 Belgrade, Serbia (e-mail: milovan.d.kovacevic@gmail.com).

$$\langle v_D \rangle_{T_S} = D V_{IN}$$
$$\langle i_D \rangle_{T_S} = (1-D)\langle i_L \rangle_{T_S} \tag{9}$$

and

$$\langle v_S \rangle_{T_S} = (1-D) V_{IN}$$
$$\langle i_S \rangle_{T_S} = D\langle i_L \rangle_{T_S} \tag{10}$$

Values of voltage and current on the input of the switching network are V_{IN} and $D\langle i_L \rangle_{T_S}$, and on its output DV_{IN} and $\langle i_L \rangle_{T_S}$, respectively. Nonlinear, time-variant switching network after averaging becomes linear, time-invariant two-port element, the ideal transformer. This fact greatly simplifies analysis of DC-DC converters. In Fig. 3, the averaged circuit of buck converter is presented.

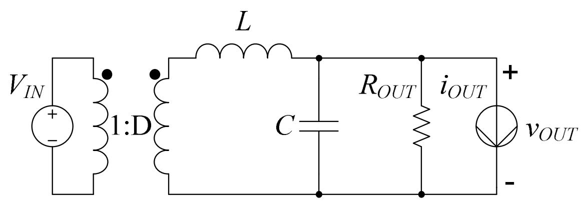

Fig. 3. Averaged circuit of buck converter.

However, input voltage v_{IN}, output current i_{OUT}, and control variable d may not be constants

$$v_{IN}(t) = V_{IN_0} + \hat{v}_{IN}(t) \tag{11}$$

$$i_{OUT}(t) = I_{OUT_0} + \hat{i}_{OUT}(t) \tag{12}$$

$$d(t) = D_0 + \hat{d}(t) \tag{13}$$

where $\hat{v}_{IN}(t)$, $\hat{i}_{OUT}(t)$ and $\hat{d}(t)$ represent variable parts of v_{IN}, i_{OUT}, and d, respectively. According to (11) and (13), input voltage transferred to the secondary side of the ideal transformer may be presented as

$$d(t)v_{IN}(t) = D_0 V_{IN_0} + D_0 \hat{v}_{IN}(t) + V_{IN_0}\hat{d}(t) + \hat{v}_{IN}(t)\hat{d}(t)\,. \tag{14}$$

Usually, the term $\hat{v}_{IN}(t)\hat{d}(t)$ is much smaller than the other terms in this sum, and may be neglected, because $\hat{v}_{IN}(t) << V_{IN_0}$, and $\hat{d}(t) << D_0$. Effectively, linearization is introduced into already averaged circuit and further simplifies analysis - converter may now be analyzed in *s*-domain.

In Fig. 4, averaged and linearized circuit in *s*-domain is presented. Without any loss of generality, factors $D_0 V_{IN_0}$ and I_{OUT_0} may be excluded from further analysis [1]. They have no effect on model's dynamics, only on the position of the bias point.

According to (12), (14), and Fig. 4, there are three independent sources: input voltage, control and output current. Also, there is one output signal, output voltage. Therefore, three transfer functions may be obtained:
control – to – output voltage transfer function

$$G_{C2OV}(s) = \frac{v_{OUT}(s)}{d(s)} = \frac{\frac{V_{IN}}{LC}}{s^2 + \frac{1}{CR_{OUT}}s + \frac{1}{LC}} \tag{15}$$

input voltage – to – output voltage transfer function

$$G_{IV2OV}(s) = \frac{v_{OUT}(s)}{v_{IN}(s)} = \frac{\frac{D_0}{LC}}{s^2 + \frac{1}{CR_{OUT}}s + \frac{1}{LC}} \tag{16}$$

and output current – to – output voltage transfer function

$$G_{OC2OV}(s) = \frac{v_{OUT}(s)}{i_{OUT}(s)} = -\frac{\frac{1}{C}s}{s^2 + \frac{1}{CR_{OUT}}s + \frac{1}{LC}}\,. \tag{17}$$

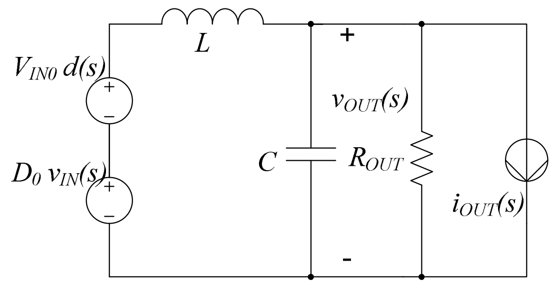

Fig. 4. Buck converter model based on averaging and linearization. Constant sources $D_0 V_{IN_0}$ and I_{OUT_0} are excluded - they have no effect on converter's dynamics.

These transfer functions are very similar - (15) and (16) are the same equation with different multiplicative factor, while (17) is their first derivative. Therefore, further analysis in this paper considers (15) only.

Let us define coefficients

$$a = \frac{1}{CR_{OUT}} \tag{18}$$

$$b = \frac{1}{LC} \tag{19}$$

and normalize (15) with $V_{IN_0}^{-1}$

$$g_{C2OV}(s) = \frac{G_{C2OV}(s)}{V_{IN_0}} \tag{20}$$

so we may write (15) in more compact form

$$g_{C2OV}(s) = \frac{b}{s^2 + as + b}\,. \tag{21}$$

III. Analysis of Effects of Discretization

In time domain, the first derivative is equivalent to multiplication with complex variable *s* in *s*-domain

$$\frac{dx(t)}{dt} \to sX(s) \tag{22}$$

where $X(s) = \mathcal{L}\{x(t)\}$. For sufficiently small time step Δt, the first derivative may be approximated with finite difference

$$f(x,t) = \frac{dx(t)}{dt} \approx \frac{\Delta x(t)}{\Delta t}, \tag{23}$$

which gives

$$\Delta x(t) \approx \Delta t\, f(x,t)\,. \tag{24}$$

For discrete time domain, three simple variations of (24) may be obtained [2]

$$x(n+1) = x(n) + T_S f(x,n) \tag{25}$$

$$x(n+1) = x(n) + T_S f(x,n+1) \tag{26}$$

and

$$x(n+1) = x(n) + T_S \frac{f(x,n) + f(x,n+1)}{2}. \tag{27}$$

Equations (25), (26), and (27) represent forward Euler, backward Euler, and trapezoidal rule for numerical integration. It may be shown that these rules are equivalent to approximations of complex variable s [3]

$$s \approx \frac{z-1}{T_S} \Leftrightarrow z \approx 1 + sT_S \tag{28}$$

$$s \approx \frac{1-z^{-1}}{T_S} \Leftrightarrow z^{-1} \approx 1 - sT_S \tag{29}$$

and

$$s \approx \frac{2}{T_S}\frac{z-1}{z+1} \Leftrightarrow z \approx \frac{1+sT_S/2}{1-sT_S/2} \tag{30}$$

respectively, where T_S is discretization/switching period.

By substituting (28), (29) and (30) in (21), three approximations of discrete transfer function are obtained:

$$g_{vd1}(z) = \frac{bT_S^2}{(z-1)^2 + aT_S(z-1) + bT_S^2} \tag{31}$$

$$g_{vd2}(z) = \frac{bT_S^2 z^2}{(z-1)^2 - aT_S z(z-1) + bT_S^2 z^2} \tag{32}$$

and

$$g_{vd3}(z) = \frac{b\frac{T_S^2}{4}(z+1)^2}{(z-1)^2 + a\frac{T_S}{2}(z^2-1) + b\frac{T_S^2}{4}(z+1)^2} \tag{33}$$

Approximations (28), (29) and (30) predict different positions of zeros and poles of discrete transfer function. Variations of pole predictions are small. However, it does not guarantee small variations in dynamic behavior of discrete model.

In Fig. 5 and Fig. 6, step responses of normalized continuous system and its discrete approximations are presented. For Fig. 5, circuit parameters are $L = 100\ \mu\text{H}$, $C = 1\ \text{mF}$, $R = 2\ \Omega$, and $T_S = 10\ \mu\text{s}$, thus giving values of model parameters $a = 10^3$ and $b = 10^7$. For Fig. 4, circuit parameters are the same except for $R = 10\ \Omega$, which gives $a = 10^2$. $d(t) = 0.5h(t)$.

Inductance L and capacitance C define corner frequency of converter's output filter

$$f_P = \frac{1}{2\pi\sqrt{LC}} = 503.3\ \text{Hz}. \tag{34}$$

Switching frequency f_S is needed to be at least 6-7 times greater than the corner frequency of the output filter [4]. In this example, $f_S = 100\ \text{kHz}$, and this "rule of thumb" is more than satisfied.

In Fig. 5 difference between step responses of discrete models is small, but visible. Models exhibit the same decaying oscillatory behavior, but with different damping factor.

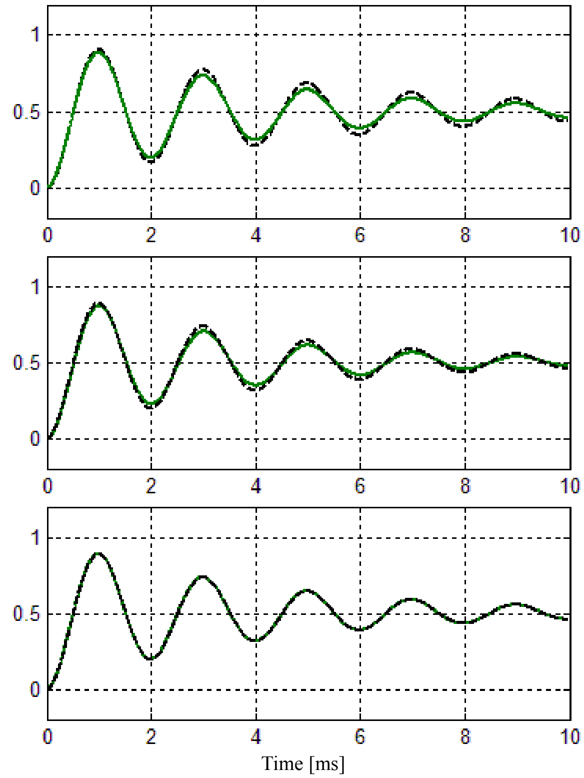

Fig. 5. Step responses of continuous model (black, --), and discrete (green) models of buck converter for $R = 2\,\Omega$.

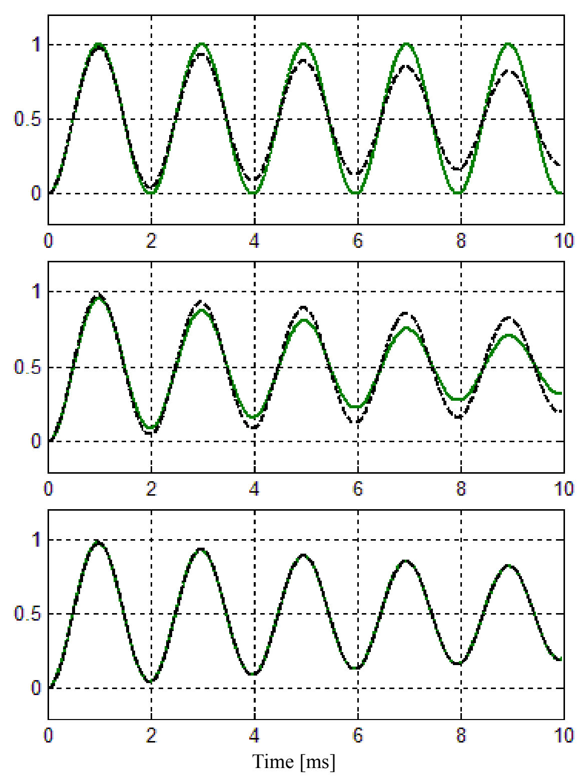

Fig. 6. Step responses of continuous model (black, --) and discrete (green) models of buck converter for $R = 10\,\Omega$.

Trapezoidal rule based model exhibits almost identical response as the continuous model, and accurately predicts the damping factor.

In Fig. 6, however, it may be observed that difference is more critical. Euler forward rule based model is boundary stable, while Euler backward rule gives inaccurate prediction for the damping factor. For $R \to \infty$, Euler backward rule based model still shows stable operation of the converter, while in reality it may be unstable or boundary stable. And again, trapezoidal rule gives almost the same prediction of system behavior as the continuous model.

To find an explanation, let us calculate the poles and their modules for Euler and trapezoidal approximations

$$\left|z_{p[EF]}\right| = \left|0.9995 \pm j0.0316\right| = 1 , \tag{35}$$

$$\left|z_{p[EB]}\right| = \left|0.9985 \pm j0.0316\right| = 0.9990 , \tag{36}$$

and

$$\left|z_{p[T]}\right| = \left|0.9990 \pm j0.0316\right| = 0.9995 . \tag{37}$$

Forward Euler rule predicts pole placement on unit circle for Fig. 4. Backward Euler rule predicts lower damping factor than trapezoidal rule. Pole positions of continuous model transferred into z-domain via step-invariant transform [4] are

$$z_{p[C]} = e^{s_{p[C]}T_S} = 0.9990 \pm j0.0316 . \tag{38}$$

It may be observed that predictions of step-invariant transform and trapezoidal rule are identical for lower frequencies.

Let us derive magnitude of pole position error introduced by Euler rules and trapezoidal rule utilizing second order Taylor series

$$z_p = e^{s_pT_S} = 1 + s_pT_S + \frac{{s_p}^2T_S^2}{2} + \dots , \tag{39}$$

$$z_p^{-1} = e^{-s_pT_S} = 1 - s_pT_S + \frac{{s_p}^2T_S^2}{2} - \dots , \tag{40}$$

and

$$z_p = \frac{e^{sT_S/2}}{e^{-sT_S/2}} = \frac{1 + \frac{s_pT_S}{2} + \frac{(s_pT_S)^2}{8} + \dots}{1 - \frac{s_pT_S}{2} + \frac{(s_pT_S)^2}{8} - \dots} . \tag{41}$$

Substituting (28) and (29) in (39) and (40) with $z = z_p$, error magnitude of pole position for Euler rules is obtained

$$error_{EF} = \left|e^{s_pT_S} - (1 + s_pT_{SE})\right| \cong \left|\frac{(s_pT_{SE})^2}{2}\right| , \tag{42}$$

and

$$error_{EB} = \left|e^{-s_pT_S} - (1 - s_pT_{SE})\right| \cong \left|\frac{(s_pT_{SE})^2}{2}\right| . \tag{43}$$

for $s_pT_{SE} << 1$. Magnitude of error introduced by both rules is of the same order. Magnitude of the error introduced by trapezoidal rule is obtained by balancing (41) with (30)

$$error_T = \left|e^{s_pT_{ST}/2}\left(1 - \frac{s_pT_{ST}}{2}\right) - e^{-s_pT_{ST}/2}\left(1 + \frac{s_pT_{ST}}{2}\right)\right| \tag{44}$$

$$error_T = \frac{2}{3}\left|\frac{(s_pT_{ST})^3}{8}\right| \tag{45}$$

Clearly, the error introduced by trapezoidal rule is much smaller than that introduced by Euler methods.

For fixed error magnitude, switching frequency for Euler rules may be found as a function of trapezoidal rule switching frequency. For $f_p = 503.3$ Hz and $T_{ST} = 10$ µs error introduced by trapezoidal rule is

$$error_T = \frac{2}{3}\left|\frac{(2\pi f_pT_{ST})^3}{8}\right| = 2.6354 \cdot 10^{-6} . \tag{46}$$

If $error_T = error_E$, switching frequency for Euler rules is obtained

$$T_{SE} = \frac{\sqrt{2error_T}}{2\pi f_p} = 726 \text{ ns} . \tag{47}$$

In this case, switching frequency for Euler rules has to be more than 10 times higher than switching frequency for trapezoidal rule for the same error magnitude. Clearly, the model of DC-DC converter based on trapezoidal rule is superior to models based on Euler rules.

IV. Conclusion

Derivation and analysis of discrete transfer function of DC-DC converters using Euler forward, Euler backward and trapezoidal rule is presented in this paper. It is shown that pole position error, introduced by discretization based on Euler rules, may have a large effect on prediction of the system behavior. Trapezoidal rule is superior to both Euler rules – it correctly predicts the system behavior and position of poles of discrete system at lower frequencies. It may have a significant effect on compensator design for DC-DC converter.

References

[1] R. W. Erricson, and D. Maksimović, "Fundamentals of Power Electronics", 2nd ed. Springer Science and Business Media, LLC, 2001.

[2] D. Tošić, "Numericka Analiza", 1st ed. Akademska Misao, 2004.

[3] Ž. Đurović, "Sistemi Automatskog Upravljanja", 1st ed. Akademska Misao, 2006.

[4] A. Prodić, "Digital Control of Switching Converters, Design and VLSI/DSP Implementation", PhD Thesis, 2003.

[5] M. Popović, "Digitalna Obrada Signala", 3rd ed. Akademska Misao, 2003.